

# A Transceiver Design of VHF Band Standardized Broadband Mobile Communications Systems

Kiminobu Makino, Keiichi Mizutani, Takeshi Matsumura, and Hiroshi Harada

Graduate School of Informatics, Kyoto University, Yoshida-honmachi, Sakyo-ku, Kyoto, 606-8501 Japan  
makino@dco.cce.i.kyoto-u.ac.jp, {mizutani, takeshi.matsumura, hiroshi.harada}@i.kyoto-u.ac.jp

**Abstract**—This paper evaluates BER performance of VHF band broadband mobile communication systems standardized as ARIB STD-T103 mode 1. The ARIB STD-T103 mode 1 is based on IEEE 802.16-2009 standard with OFDMA because of its easy implementation. The IEEE 802.16-2009 based system is originally expected to operate in microwave bands such as 2.5 GHz with 512 FFT based OFDM in 5 MHz channel. However, the ARIB STD-T103 based system should tune the radio parameters of IEEE 802.16-2009 to suit for VHF band propagation characteristics because many multipath waves with long delay path are received in the VHF band. The ARIB STD-T103 mode 1 adopts OFDMA with 1024 FFT in 5 MHz channel and convolutional Turbo coding to cope with long delay multipath environments in VHF band such as IEEE 802.22 Profile A model. However, the BER performance in the environments has never been evaluated. This paper evaluates the BER performance with conventionally proposed receiving scheme by computer simulation. However, the performances of UL and DL with 64QAM do not achieve the required BER of ARIB STD-T103. To improve the BER performance this paper proposes three channel estimation schemes for DL. Although the BER performance with the schemes are not improved drastically, it is clarified that one of the proposals is expected to reduce size of storage in comparison with the conventional estimation schemes. With the estimation scheme and maximum ratio combined diversity achieves the required BER in both UL and DL.

**Keywords**—IEEE 802.16, ARIB STD-T103, VHF, Broadband, OFDMA

## I. INTRODUCTION

Recently the 5th generation wireless communication (5G) systems have been researched and developed to cope with explosive growth of wireless communication traffic. In 5G era, carrier aggregation and heterogeneous network over different frequency bands as well as in one frequency band will be activity used. This is because the requirement for the 5G systems is not only high data rate communications but also collaboration of multiple services such as very high data communications and very low data rate sensing data communications.

One of the solutions to realize the multiple services collaboration is the adaptive collaboration of frequency band, cell size, and transmission scheme. For example, the small size cell with 100 m - 2 km radius service area using higher frequency bands, e.g. microwave band, millimeter wave band or so on is allocated to the relatively higher data rate communications. The size is small, however the high data rate

and dense communication services can be provided by establishing many base stations (BSs). On the other hand, the large size cell with several km is prepared by using lower frequency bands, e.g. VHF band is allocated. The size is longer than that by using the microwave or higher frequency bands. This large cell service might be suitable for the broadcasting or uni-casting of the control signals for cellular phone user (C-plane).

Another solution to use multiple services is Internet-of-Things (IoT). In the coverage area with at most several km, sensing information such as environmental sensing information, medical sensing information, or machine monitoring information is collected by using sensor networks with low transmission speed such as several hundred kbps and the sensing information is transmitted to data concentrator. The data concentrator is connected with data collection server through wide area network with coverage area of several tens km as backhaul communication network. VHF band is one of candidate frequencies for the network.

In Japan, the analog TV broadcasting services in VHF band (170 MHz – 202.5 MHz) were finished in 2012. The VHF band becomes a kind of TV white space and reassigned for broadband wireless communication systems with 5 MHz channel bandwidth [1]. In accordance with these circumstances, several wireless specifications of the VHF broadband communication systems have already been standardized in Japan.

ARIB STD-T103 [2] by association of radio industries and businesses (ARIB) of Japan is the example. The ARIB STD-T103 is based on IEEE 802.16-2009 standard [3] with OFDMA because IEEE 802.16-2009 based system is a wide area network (WAN) with at least one base station (BS) and several mobile stations (MSs), and does not need complicated core network like 3GPP based system and it is easily introduced to several applications. The IEEE 802.16-2009 based system is originally expected to operate in microwave bands such as 2.5 GHz as WiMAX™ with 512 FFT based OFDM. By operating it in VHF bands, it may cover wider area in comparison with that in microwave bands. However, the ARIB STD-T103 based system should tune its radio parameters of IEEE 802.16-2009 to suit for VHF band propagation characteristics because many multipath waves with long delay path are received in the VHF bands. Several channel characteristics in the VHF bands were reported. In [4][5], there are possibility to receive multipath waves with

maximum delay time greater than 20 us. Also channel models are defined in IEEE 802.22 standard project that pursues wireless regional area network with several tens km in TV white space (TVWS) bands such as VHF and UHF to evaluate performance of the transceiver. For example, maximum delay time of IEEE 802.22 profile A model is 21 us [6]. The FFT size and subcarrier spacing of IEEE 802.16-2009 based OFDMA system operating in the bandwidth of 5MHz/channel is 512 and 10.94 kHz, respectively [3]. In this case, the cyclic prefix (CP) duration is 11.5 us when cyclic prefix is assumed as 1/8 of the effective OFDM symbol duration. It means that it is impossible to cover wider area when conventional IEEE 802.16-2009 based system in microwave band is just frequency-converted to VHF band because the cyclic prefix duration is smaller than maximum delay time of multipath waves in VHF band. To resolve the issues above, the ARIB STD-T103 based system tunes the radio parameters of IEEE 802.16-2009 to suit for VHF band propagation characteristics. The ARIB STD-T103 adopts OFDM transmission with 1024 FFT and subcarrier spacing of 5.47 kHz in 5 MHz channel and convolutional code and convolutional Turbo code (CTC). However, the BER performance of the ARIB STD-T103 in the long delay multipath environments in VHF band such as IEEE 802.22 Profile A has never been evaluated.

This paper firstly introduces ARIB STD-T103 mode 1 based on IEEE 802.16-2009. Then, this paper evaluates the BER performance with conventionally proposed receiving scheme by computer simulation. However, the performances of UL and DL with 64QAM do not achieve the required BER of ARIB STD-T103. To improve the BER performance, this paper proposes three channel estimation schemes for DL. Although the BER performances with the schemes are not improved drastically, it is clarified that one of the proposals is expected to reduce size of storage in comparison with the conventional estimation schemes. With the estimation scheme and maximum ratio combined diversity achieves the required BER in both UL and DL.

## II. ARIB STD-T103 MODE 1

The specification of ARIB STD-T103 mode 1 is summarized in Table I. The ARIB STD-T103 mode 1 has two modes: mode 1 (FFT size =512) and mode 1 (FFT size = 1024). The channel bandwidth, modulation scheme, multiple access scheme, duplex method, maximum transmission (Tx) power, pilot pattern and MAC layer protocol are same in both modes on the basis of IEEE 802.16-2009. The differences between two modes are mainly five points: FFT size, frame length, OFDM symbol length, cyclic prefix length. Especially mode 1 (FFT size = 1024) can support delayed waves with greater than 20 ns. In addition to the above differences, mode 2 only has a unique function. This is slot allocation ratio for downlink and uplink in a TDD frame. The mode 1 can support only 35:21 and 26:21 as an occupation ratio of a TDD frame for downlink and uplink. However, the mode 1 (FFT size = 1024) can support an additional ratio of 9:38. This means that the mode can give a high priority of uplink and is effective for

the use cases such as disaster monitoring, environment monitoring and surveillances.

TABLE I SPECIFICATIONS OF ARIB STD-T103 MODE 1.

		Parameter				
Base standard	Wireless MAN-OFDMA (IEEE 802.16e)					
Channel Bandwidth	5.0 MHz					
Modulation scheme	QPSK, 16QAM, 64QAM					
Multiple access	DL : OFDM/TDM, UL : OFDMA					
Duplex method	TDD					
Tx power	5 W (37 dBm)					
FFT size	512	1024				
Subcarrier spacing	10.94 kHz	5.47 kHz				
Frame length	5.0 ms	10 ms				
OFDM symbol length	102.8 $\mu$ s	205.7 $\mu$ s				
Cyclic Prefix length	11.4 $\mu$ s	22.9 $\mu$ s				
DL:UL	35:12	26:21	35:12	26:21	9:38	
DL-tx rate [Mbps]	6.3	4.3	6.3	4.3	0.65	
UL-tx rate [Mbps]	1.5	3.0	1.5	3.0	5.9	
Pilot pattern	IEEE 802.16-2009					
MAC	IEEE 802.16-2009					

## III. CONFIGURATION OF TRANSMITTER

### A. Overview

Fig. 1 shows a transmitter block diagram of ARIB STD-T103 based system. In the transmitter, firstly channel coding, interleaving and modulation are performed on the transmission binary data in channel coding and modulation function block before dividing into subchannels for each user. The coded and modulated subchannel I/Q data symbols are allocated to each subcarrier with pilot and null symbols in the partial usage of subchannels (PUSC) mapping function block. Finally, IFFT is performed on the subcarriers and CP is added to the IFFT performed signals in time domain to reduce inter-symbol-interference caused by multipath fading. As shown in Table II, the number of data, pilot, and null subcarriers are different between the cases of downlink (DL) and uplink (UL).

### B. Channel Coding and Modulation

Channel coding and modulation in Fig. 1 include data randomization, forward error correction (FEC), interleaving and modulation processes. CTC is a candidate of the coding scheme in ARIB STD-T103. After CTC channel coding, to change the coding rate as 1/2, 3/4 and 2/3, a puncturing process is performed. Modulation scheme for the transmission data can be selected from QPSK, 16QAM and 64QAM. Modulation scheme for the pilot data is only BPSK.

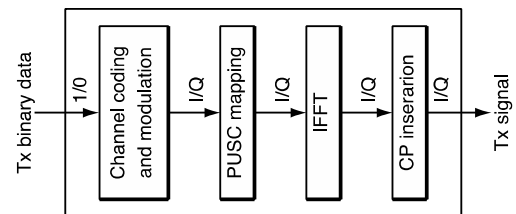


Fig. 1. A structure of transmitter.

### C. PUSC mapping

#### 1) DL-PUSC

Firstly, the PUSC mapping process of DL is explained. Fig. 2 shows the DL-PUSC mapping procedure. In the DL-

PUSC, 720 subcarriers in one OFDM symbol are divided into 30 groups, i.e. each group has 24 subcarriers. The each group makes 30 subchannels with adjacent OFDM symbol, i.e. each subchannel has 48 subcarriers as shown in Fig. 3. These 30 subchannels are divided into 6 major groups. The  $n^G$ -th and  $(n^G + 1)$ -th major groups have 6 and 4 subchannels respectively, where  $n^G \in 0, 2, 4$ . The  $k$ -th subcarrier in the  $s$ -th major group is allocated to the  $n_{k,s}^{\text{SC}}$ -th subcarrier as

$$\begin{aligned} n_{k,s}^{\text{SC}} &= N^G n_k + \{p_s [n_k \bmod N^G \\ &\quad + N^{\text{DLPB}}] \bmod N^G \\ n_k &= (k + 13 \cdot s) \bmod N^G \\ k &= \begin{cases} 0, 1, \dots, 143 & (n^G \bmod 2 = 0) \\ 0, 1, \dots, 95 & (n^G \bmod 2 = 1) \end{cases} \end{aligned} \quad (1)$$

where  $N^G = 6$  is number of major groups,  $p_s$  is allocation sequence with rotation factor  $s$  in each major group, and  $0 < N^{\text{DLPB}} < 31$  is parameter in DL-MAP which is selected in control layer. After that, subcarriers are divided into clusters. Each cluster is composed of 14 subcarriers and two OFDM symbols, i.e. one cluster has 28 data subcarriers as shown in Fig. 2. The  $n^{\text{LC}}$ -th cluster is re-allocated to the  $n^{\text{PC}}$ -th cluster as

$$n^{\text{LC}} = \text{RS}\{(n^{\text{PC}} + 13 \times N^{\text{DLPB}}) \bmod N^{\text{CL}}\}, \quad (2)$$

where  $N^{\text{CL}} = 60$  is number of clusters and  $\text{RS}\{\cdot\}$  is re-allocated sequence for clusters. Finally, four pilot subcarriers modulated by boosted-BPSK are added to each cluster.

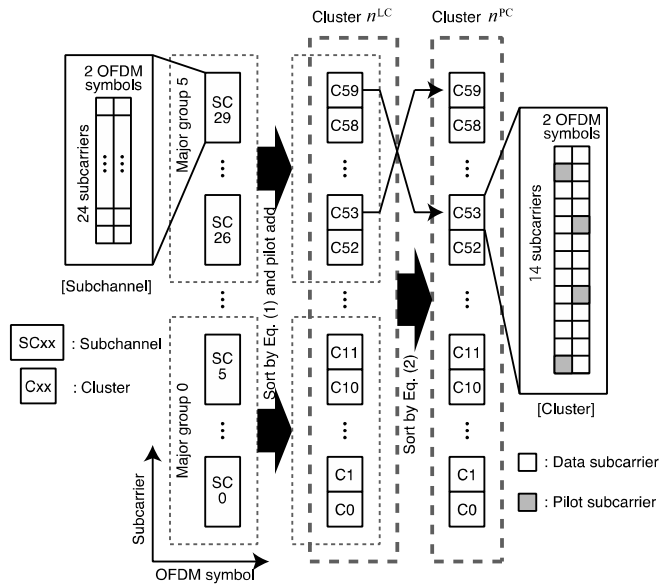


Fig. 2. DL-PUSC mapping procedure.

## 2) UL-PUSC

Fig. 3 shows the UL-PUSC mapping procedure. In the UL-PUSC, one OFDM symbol has 840 subcarriers. Three adjacent OFDM symbols are aggregated and divided into 210 tiles, i.e. each tile has 12 subcarriers including 4 pilot subcarriers and 8 data subcarriers as shown in Fig. 3. These 210 tiles are aggregated as 35 subchannels, i.e. each subchannel has six tiles. Firstly, subchannel number is rotated by 13. The  $m$ -th subchannel before subchannel-rotation is allocated to the  $s$ -th subchannel as

$$s = (m + 13) \bmod N^{\text{Sch}}, \quad (3)$$

where  $N^{\text{Sch}} = 35$  is number of subchannels. Each subchannel is divided into tiles. The  $n_c$ -th subcarrier in the  $s$ -th subchannel is numbered with  $n_{c,s}^{\text{SC}}$  as

$$n_{c,s}^{\text{SC}} = (n_c + 13 \cdot s) \bmod N^{\text{SCa}}, \quad (4)$$

where  $N^{\text{SCa}} = 48$  is number of data subcarriers in one subchannel. That the  $n_t$ -th tile in  $s$ -th subchannel is reallocated to the  $n_{s,t}^{\text{tile}}$ -th tile as

$$\begin{aligned} n_{s,t}^{\text{tile}} &= N^{\text{Sch}} \cdot n_t \\ &\quad + (P_t [(s + n_t) \bmod N^{\text{Sch}}] \\ &\quad + N^{\text{ULPB}}) \bmod N^{\text{Sch}}, \end{aligned} \quad (5)$$

where  $P_t$  is allocation sequence for tiles. Finally, pilot subcarriers modulated by BPSK is added.

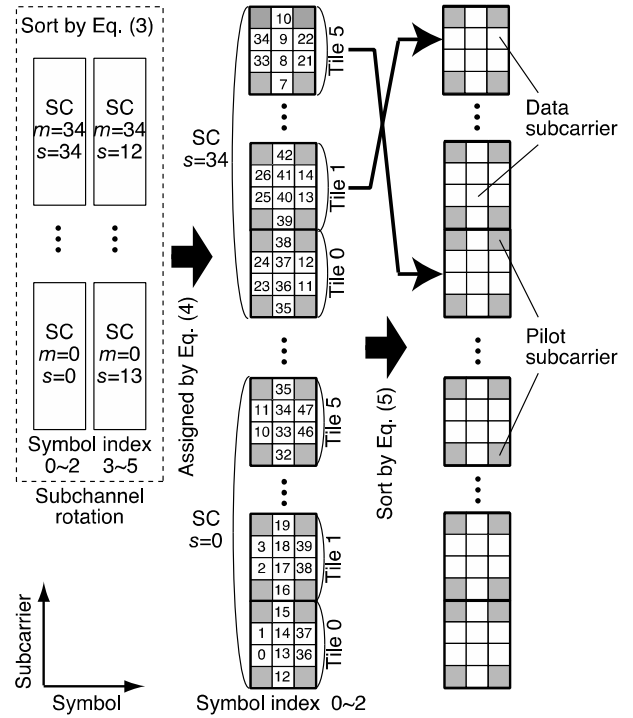


Fig. 3. UL-PUSC mapping procedure.

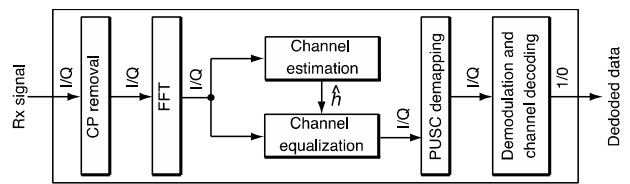


Fig. 4. A structure of receiver.

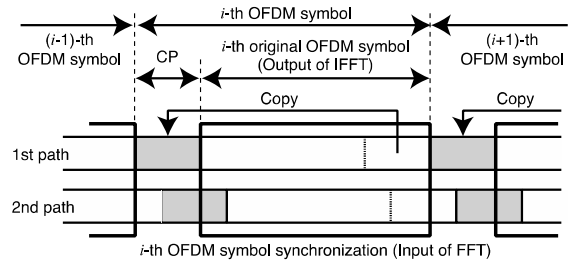


Fig. 5. OFDM demodulation process.

TABLE II NUMBER OF SUBCARRIERS.

	DL	UL
No. of null subcarriers	184	
No. of pilot subcarriers	120	280
No. of data subcarriers	720	560

#### IV. CONFIGURATION OF RECEIVER

##### A. Overview

Fig. 4 shows a receiver block diagram of ARIB STD-T103. Firstly, each CP which is removed before obtaining received subcarriers by FFT processing as shown in Fig. 5. If the CP length is appropriate to remove the effect of delay paths, there are no inter-symbol interference (ISI) and inter-carrier interference (ICI) in the obtaining subcarriers. After the FFT processing, channel estimation, equalization, and demapping to subchannels are performed. Finally, demodulation and channel decoding are performed.

##### B. Channel Estimation and Equalization

The received subcarrier is expressed by

$$r_{i,j} = h_{i,j} s_{i,j} + n_{i,j}, \quad (6)$$

where  $s_{i,j} \in \mathbb{C}$ ,  $r_{i,j} \in \mathbb{C}$ ,  $h_{i,j} \in \mathbb{C}$  and  $n_{i,j} \in \mathbb{C}$  represent transmitted signal, received signal, effective channel including multipath propagation channel and effect of transceiver weight, e.g. IFFT, CP insertion/removal and FFT, and noise of the  $j$ -th subcarrier in the  $i$ -th OFDM symbol, respectively. By using pilot subcarriers  $s_{p,q_p}$ , which are known signal at both of transmitter and receiver, the effective channel  $\hat{h}_{p,q_p}$  is obtained as following,

$$\hat{h}_{p,q_p} = \frac{r_{p,q_p}}{s_{p,q_p}} = h_{p,q_p} + \frac{n_{p,q_p}}{s_{p,q_p}}, \quad (7)$$

where  $q_p \in Q_p$  and  $Q_p$  represents pilot subcarrier index in the  $p$ -th OFDM symbol. The effective channel  $\hat{h}_{i,j}$  of data subcarriers is estimated by interpolation or extrapolation using these obtained effective channel of pilot subcarriers  $\hat{h}_{p,q_p}$ . To equalize the effective channel and getting the transmitted data subcarriers  $s_{i,j}$ , the received data subcarriers  $r_{i,j}$  are multiplied by inverse of estimated effective channel  $\hat{h}_{i,j}$ . Several channel estimation methods for IEEE 802.16-2009 pilot patterns have been studied [6] - [11]. This paper focuses on only linear interpolation and extrapolation based channel estimation scheme to reduce complexity.

##### C. Channel Estimation in UL

Due to the difference of the structures of transmission subcarrier unit in UL and DL, i.e. the subcarrier tile structure in UL and the subcarrier cluster structure in DL as shown in Figs. 6 and 7, different  $\hat{h}_{i,j}$  estimation schemes should be applied to the UL and DL systems respectively.

Since UL is multiple access based system in which each subchannel is allocated to each user, each subchannel allocated to each user is received at BS via different paths respectively. Therefore, the channel estimation should be completed in each tile [11]. In this paper, this kind of channel estimation scheme completed in each subcarrier unit, i.e. tile in UL and cluster in

DL is named a unit complete type channel estimation scheme (Complete scheme). In the UL tile, four pilot subcarriers are allocated to each four corner of the tile, hence, the effective channels of the data subcarriers can be estimated by interpolating between each pilot subcarriers as shown in Fig. 6. Let us assume that the effective channel in each tile is defined as  $\tilde{h}_{s,t}^{x,z} = \hat{h}_{i,j}$ , where  $s = i \bmod 3$  and  $t = j \bmod 4$  are symbol and subcarrier index in each cluster,  $x = \lfloor i/3 \rfloor$  is the tile symbol index and  $z = \lfloor j/4 \rfloor$  is the tile subcarrier index respectively. All effective channels of the data subcarriers in the tile can be estimated by interpolating between each pilot subcarrier in frequency and time domain respectively as following,

$$\tilde{h}_{s,t}^{x,z} = \frac{1}{6} (2-s)(3-t) \tilde{h}_{0,0}^{x,z} + st \tilde{h}_{2,3}^{x,z} + s(3-t) \tilde{h}_{2,0}^{x,z} + (2-s)t \tilde{h}_{0,3}^{x,z}. \quad (8)$$

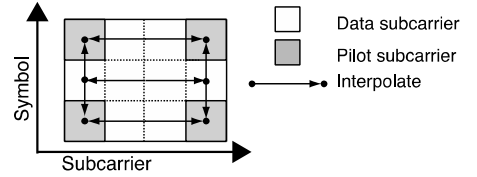


Fig. 6. A channel estimation method for UL.

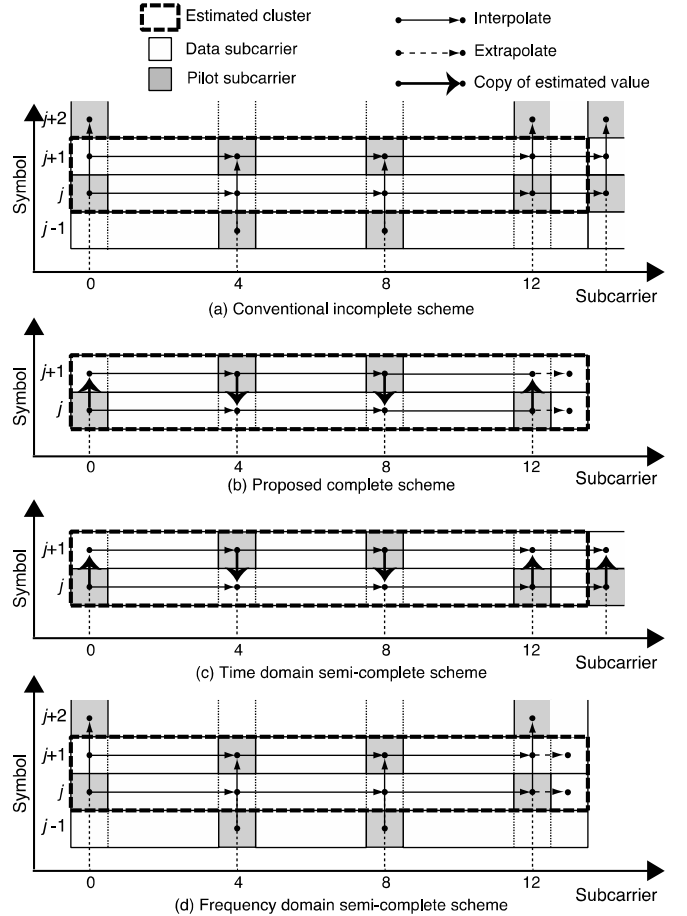


Fig. 7. Conventional and proposed channel estimation methods for DL.

#### D. Channel Estimation in DL

Since DL is broadcasting system, each user can receive all subcarriers. Therefore, each user can use all pilot subcarriers belonging to not only own clusters but also clusters for another user for estimating effective channels. In this paper, this kind of channel estimation scheme using several subcarrier units is named a unit incomplete type channel estimation scheme (Incomplete scheme). Because all pilot subcarriers including for other users can be used for channel estimation, pilot subcarriers rate can be reduced. As a result, data transmission efficiency is better than UL system. As shown in Fig. 3, three pilot subcarriers are not allocated at the corner of the cluster. Therefore, the effective channels of the data subcarriers that is not allocated between pilot subcarriers are estimated by the Incomplete scheme using pilots of the neighbor clusters in conventional scheme [6] as shown in Fig. 7(a).

#### E. Demodulation and Decoding

Fig. 8 shows the decoder design of the proposed receiver including soft-demodulation based on [12], deinterleaving, decoding and derandomizing function blocks. When CTC decoding is used, Max-Log-MAP [13] based algorithm is applied.

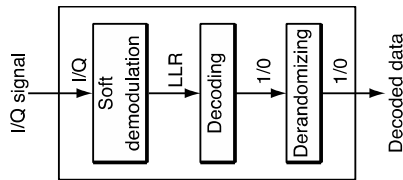


Fig. 8. A procedure of demodulation and channel decoding.

#### V. PERFORMANCE EVALUATION USED CONVENTIONAL TRANSMITTER AND RECEIVER

The transmission performance used conventional transmitter and receiver is evaluated by computer simulation in terms of signal to noise ratio (SNR) to bit-error-rate (BER). The simulation parameters are summarized in Table III. The AWGN (Additive white Gaussian noise) environment, the GSM Typical Urban model that is urban multipath fading channel model shown in Table IV and the IEEE 802.22 Profile A model that is multipath fading channel model with long delay path for the service area from 10 km standardized by IEEE 802.22 working group shown in Table V are used for the evaluation.

##### A. Performance evaluation in AWGN environment

Fig. 9 shows BER performance in the AWGN environment by computer simulation for each MCS. In the AWGN environment, DL and UL have nearly the same performances. The difference for each MCS of the SNR that achieves the required BER =  $10^{-6}$  is about 5-6 dB.

##### B. Configuration of proposed receiver in multipath fading environments

Fig. 10 shows BER performance of the UL receiver using the Complete channel estimation scheme with 64QAM in

GSM Typical Urban model and IEEE 802.22 Profile A model. The degradation from the ideal BER by the channel estimation effect can be managed within 3.0 dB in terms of SNR at BER =  $10^{-6}$  in GSM Typical Urban model. An error floor occurs in IEEE 802.22 Profile A model. This is because the pilot subcarrier interval is wide and channel estimation error is large because the frequency selectivity of fading is severe due to the long delay time.

TABLE III CONFIGURATIONS OF SIMULATION PARAMETERS.

	Simulation	Experiment
Standard	ARIB STD-T103 Mode 1	
Modulation scheme	QPSK, 16QAM, 64QAM	
FFT size	1024	
Coding rate	1/2	
Symbol rate	4.862 kHz	
CP size rate	1/8	
Channel model	AWGN environment	
	GSM Typical Urban model	
	IEEE 802.22 Profile A model	
Encoding and decoding	CTC, Max-Log MAP algorithm	
Moving speed	80 km/h ( $f_D T_s = 3 \times 10^{-3}$ )	
DL:UL	-	9:38
Max Tx power (BS)	-	5 W(37 dBm)
Max Tx power (MS)	-	1 W(30 dBm)
Frequency	-	192.5 -197.5 MHz

TABLE IV GSM TYPICAL URBAN MODEL.

Path number	1	2	3	4	5	6
Delay time [s]	-0.2	0	0.3	1.4	2.1	4.8
Relative power [dB]	-3	0	-2	-6	-8	-10

TABLE V IEEE 802.22 PROFILE A MODEL.

Path number	1	2	3	4	5	6
Delay time [s]	0	3.0	8.0	11	13	21
Relative power [dB]	0	-7.0	-15	-22	-24	-19

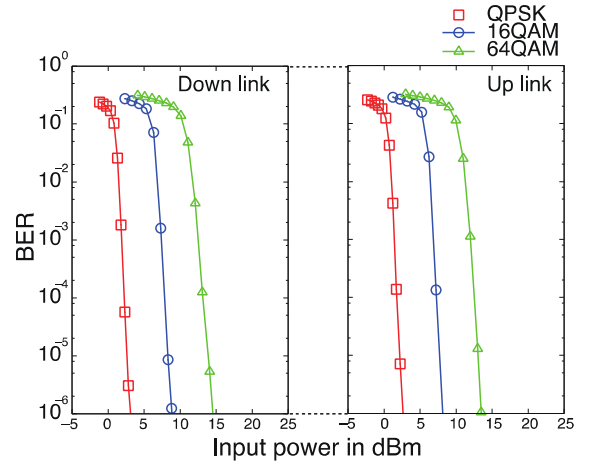


Fig. 9. BER performance in AWGN environment.

Fig. 11 shows BER performance of the DL receiver using conventional channel estimation schemes include the conventional scheme with 64QAM in GSM Typical Urban model. The BER degradation of the proposed Complete scheme is 1.5 dB compared to the ideal case in terms of SNR at BER =  $10^{-6}$ . As a result, in the GSM Typical Urban model, the channel estimation error degrades the BER

performance.

Fig. 12 shows BER performance of the DL receiver using conventional channel estimation schemes with 64QAM in IEEE 802.22 Profile A model. With the estimation scheme, error floor occurs and the performance does not achieve the required BER of  $10^{-6}$ . From the above results, we should consider the channel estimation scheme again.

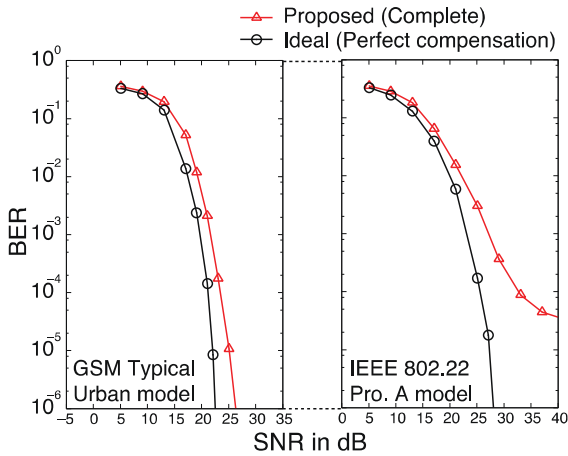


Fig. 10. BER performance of UL channel estimation.

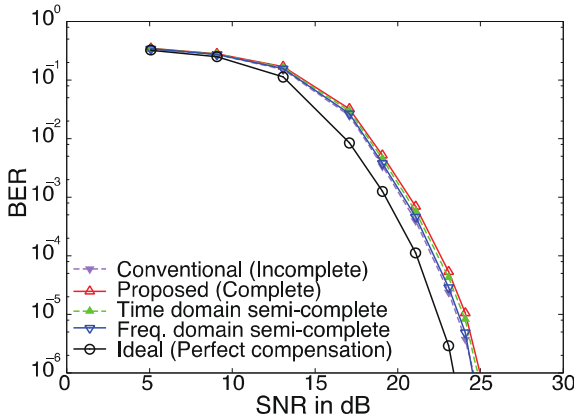


Fig. 11. BER performance of DL channel estimation in GSM Typical Urban model.

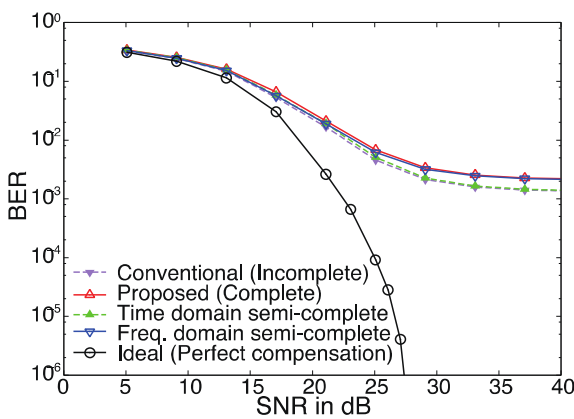


Fig. 12. BER performance of DL channel estimation in IEEE 802.22 Profile A model.

## VI. PROPOSAL TO ACHIEVE REQUIRED BER IN MULTIPATH FADING ENVIRONMENTS AND TO DEVELOP ACTUAL RADIO EQUIPMENT

### A. Channel estimation scheme

The receiver used in conventional channel estimation in DL does not achieve the required BER of  $10^{-6}$  when 64QAM-OFDM is selected. Moreover, as shown in Fig. 7(a), the conventional channel estimation uses the pilot subcarriers of neighbor clusters. It is necessary to store information other than the subcarriers of user's cluster. To develop actual radio equipment, we need simple channel estimation schemes that keep almost same BER performance with the conventional scheme and not to store information other than the subcarriers of user's cluster.

This paper proposes a Complete scheme for DL cluster structure shown in Fig. 7 (b). This paper also evaluates two types Semi-complete schemes named Frequency domain and Time domain semi-complete schemes respectively. The Time domain semi-complete scheme shown in Fig. 7 (c) uses a pilot subcarriers of neighbor cluster in only frequency domain, i.e. this scheme is the Complete scheme in time domain and the Incomplete scheme frequency domain.

In contrast, the Frequency domain semi-complete scheme shown in Fig. 7 (d) uses a pilot subcarriers of neighbor cluster in only time domain. Let us assume that the effective channel in each cluster is defined as  $\tilde{h}_{s,t}^{x,z} = \hat{h}_{i,j}$ , where  $s = i \bmod 2$  and  $t = j \bmod 14$  are symbol and subcarrier index in each cluster,  $x = \lfloor i/2 \rfloor$  is the cluster symbol index and  $z = \lfloor j/14 \rfloor$  is the cluster subcarrier index respectively. These four channel estimation schemes including the conventional and proposed scheme are performed by time domain and frequency domain estimation stages.

Firstly, the procedure of the time domain estimation stage is explained. In the conventional and the Frequency domain semi-complete schemes, the effective channels of two neighbor symbols in one cluster are estimated by interpolating between pilots of the own cluster and the pilots of the neighbor cluster as follows,

$$\begin{aligned} \tilde{h}_{1,t}^{x,z} &= \frac{1}{2} \{ \tilde{h}_{0,t}^{x,z} + \tilde{h}_{0,t}^{x+1,z} \} \quad (t = 0, 12) \\ \tilde{h}_{0,t}^{x,z} &= \frac{1}{2} \{ \tilde{h}_{1,t}^{x,z} + \tilde{h}_{1,t}^{x-1,z} \} \quad (t = 4, 8). \end{aligned} \quad (9)$$

On the other hand, in the proposed Complete and the Time domain semi-complete schemes, these effective channels are the same and the neighbor effective channels of the pilots in time domain are estimated by copying of the estimated effective channels of the pilots as follows,

$$\begin{aligned} \tilde{h}_{1,t}^{x,z} &= \tilde{h}_{0,t}^{x,z} \quad (t = 0, 12) \\ \tilde{h}_{0,t}^{x,z} &= \tilde{h}_{1,t}^{x,z} \quad (t = 4, 8). \end{aligned} \quad (10)$$

Secondly, the frequency domain estimation stage is explained. In all estimation schemes, all effective channels of the data subcarriers except the 13th subcarrier are estimated by interpolating between pilots of the own cluster as following,

$$\tilde{h}_{s,t}^{x,z} = \frac{1}{4} \left\{ t_{\text{mod}} \tilde{h}_{s,4(\lfloor \frac{t}{4} \rfloor + 1)}^{x,z} + (4 - t_{\text{mod}}) \tilde{h}_{s,4\lfloor \frac{t}{4} \rfloor}^{x,z} \right\} \quad (t = 13), \quad (11)$$

where  $t_{\text{mod}} = t \bmod 4$ . In the proposed Complete and Frequency domain semi-complete schemes, the effective channel of the 13th subcarrier is estimated by extrapolating from the estimated effective channels of the 8th and the 12th subcarriers as following,

$$\tilde{h}_{s,13}^{x,z} = \frac{1}{4} \{ 5\tilde{h}_{s,12}^{x,z} - \tilde{h}_{s,8}^{x,z} \}. \quad (12)$$

On the other hand, in the conventional and time domain semi-complete schemes, the effective channel of the 13th subcarrier are estimated by interpolating between the estimated effective channels of the 12th subcarrier of the own cluster and the 1st subcarrier of the adjacent cluster as following,

$$\tilde{h}_{s,13}^{x,z} = \frac{1}{2} \{ \tilde{h}_{s,0}^{x,z+1} - \tilde{h}_{s,12}^{x,z} \}. \quad (13)$$

In the case of  $z = 59$ , the effective channels of the 13th subcarriers are estimated by extrapolating as the same of the proposed Complete and Frequency domain semi-complete schemes.

### B. MRC diversity

Since the receiver used conventional channel estimation in DL does not achieve the required BER of  $10^{-6}$  when 64QAM-OFDM is selected and there are propagation environments in which high-speed communication cannot be performed by proposed receivers, diversity receiving technique needs to be considered by multiple antennas instead of by a single antenna. It was assumed that the maximum ratio combining diversity is applied to two receiving antennas with uncorrelated fading. By using transmission signal  $s$ , received signal and estimated effective channel of branch 1  $r_1$  and  $\tilde{h}_1$ , received signal and estimated effective channel of branch 2  $r_2$  and  $\tilde{h}_2$ , MRC and equalized signal  $r'$  is obtained as following,

$$r' = \frac{r_1 \tilde{h}_1^* + r_2 \tilde{h}_2^*}{|\tilde{h}_1|^2 + |\tilde{h}_2|^2}. \quad (14)$$

### C. Performance evaluation

Fig. 12 shows BER performance of the DL receiver using four channel estimation schemes with 64QAM in IEEE 802.22 Profile A model. With all estimation schemes, error floor occurs. The proposed Complete scheme and the Time domain semi-complete scheme have a little bit higher error floor compared to the conventional Incomplete scheme and Frequency domain semi-complete scheme. It shows that the frequency selectivity of this model strongly influences more than the time fluctuation. In the following discussion, the proposed Complete scheme is adopted as the simplest scheme. Fig. 13 shows BER performance of QPSK, 16-QAM and 64 QAM in 802.22 profile A models by the proposed channel estimation scheme. Fig. 13 also shows BER performance using MRC diversity in the IEEE 802.22 Profile A model by

computer simulation. The fading of the two signals is assumed to be completely uncorrelated. Both DL and UL solve the floor error that occur in single antenna and achieved BER =  $10^{-6}$ .

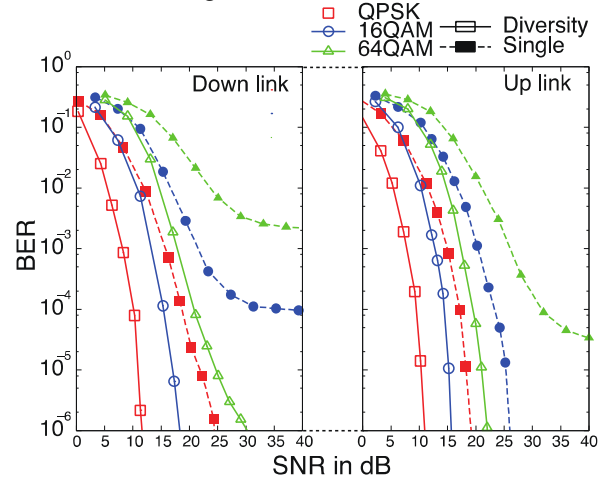


Fig. 13. Performance evaluation in 802.22 Profile A model with and without MRC diversity.

## VII. CONCLUSION

This paper evaluated BER performance of VHF band broadband mobile communication systems based on conventional ARIB STD-T103 mode 1 with conventional receiving schemes by computer simulations. The BER performance of DL with 64QAM did not achieve the required BER in the IEEE 802.22 Profile A model. To improve the BER performance, this paper proposed three channel estimation schemes for DL. By the schemes, the performances of DL with 64QAM still did not achieve the required BER in the IEEE 802.22 Profile A model. But one of the proposals, Complete scheme for DL cluster structure, was expected to reduce size of storage in comparison with the conventional estimation schemes. By using two branches MRC diversity and the proposed channel estimation scheme, the BER achieved the required BER in 802.22 Profile A model. For the future study, the development of the prototype by using our proposed channel scheme and MRC diversity is required.

## REFERENCES

- [1] M. Oodo and H. Harada, Proc. WPMC 2014, pp. 759-764, Sep. 2014.
- [2] ARIB STD-T103 Version 1.2, , Mar, 2015
- [3] IEEE std 802.16n-2013, Jun. 2013
- [4] Ming-Tuo Zhou, et al., IEEE Commun. Mag. , pp. 198-207, Aug. 2015.
- [5] IEEE std 802.16-2009, May. 2009.
- [6] M. Mohamad, et al., Proc. ICCCE 2008, pp. 1340-1343, May. 2008.
- [7] S. Galih, et al., Proc. ICEEI '09, vol. 02, pp. 478-483, Aug. 2009.
- [8] S. SU, et al., Proc. ICACT 2010, pp. 775-779, Feb. 2010.
- [9] W. Wu et al., Proc. APCC 2007, pp. 85-88, Oct. 2007.
- [10] S. Coleri, et al., IEEE Trans., vol.48, pp.223-229, Sep. 2002.
- [11] K. Ho and A. Kwasinski, Proc. WCNC 2009, pp. 1-6, Apr. 2009..
- [12] H. Harada et al., IEICE Trans. Commn., Vol. E84-B, No. 8, , Aug. 2001.
- [13] P. Robertson et al., Proc. ICC '95, Vol.2, pp.1009-1013, Jun. 1995.
- [14] W. C. Jakes, IEEE Veh. T., Vol.20, pp.81-92, Nov. 1971.